Front. Optoelectron. 2013, 6(4): 418–428
DOI 10.1007/s12200-013-0343-9

RESEARCH ARTICLE

Side chains and backbone structures influence on 4,7-dithien-2-yl-2,1,3-benzothiadiazole (DTBT)-based low-bandgap conjugated copolymers for organic photovoltaics

Debin NI[1], Dong YANG[2], Shuying MA[1], Guoli TU (✉)[1], Jian ZHANG (✉)[2]

1 Wuhan National Laboratory for Optoelectronics, School of Optical and Electronic Information, Huazhong University of Science and Technology, Wuhan 430074, China
2 State Key Laboratory of Catalysis, Dalian Institute of Chemical Physics, Chinese Academy of Sciences, Dalian National Laboratory of Clean Energy, Dalian 116023, China

Abstract Five 4,7-dithien-2-yl-2,1,3-benzothiadiazole (DTBT)-based conjugated copolymers with controlled molecular weight were synthesized to explore their optical, energy level and photovoltaic properties. By tuning the positions of hexyl side chains on DTBT unit, the DTBT-fluorene copolymers exhibited very different aggregation properties, leading to 60 nm bathochromic shift in their absorptions and the corresponding power conversion efficiencies (PCEs) value of photovoltaic cells varied from 0.38%, 0.69% to 2.47%. Different copolymerization units, fluorene, carbazole and phenothiazine were also investigated. The polymer based on phenothiazine exhibited lower PCE value due to much lower molecular weight owing to its poor solubility, although phenothiazine units were expected to be a better electron donor. Compared with the fluorene-based polymer, the carbazole-DTBT copolymer showed higher short circuit current density (J_{sc}) and PCE value due to its better intermolecular stacking.

Keywords 4,7-dithien-2-yl-2,1,3-benzothiadiazole (DTBT), conjugated polymers, low-bandgap, organic photovoltaics

1 Introduction

Organic photovoltaics (OPVs) are a promising sustainable energy source with unique advantages, such as low-cost, light weight, and flexibility [1–4]. Bulk heterojunction active layer was usually a blend of an electron-donating conjugated polymer and an electron-accepting fullerene derivative, such as [6,6]-phenyl-C_{61}-bulyric acid methyl ester ($PC_{60}BM$) [5,6] or [6,6]-phenyl-C_{71}-bulyric acid methyl ester ($PC_{70}BM$) [7–10]. Poly (3-hexylthiophene) (P3HT) has been intensively investigated as the electron donor in organic/polymer photovoltaic cells with the power conversion efficiency (PCE) up to 6.5% [11–15]. In the past few years, a lot of works were focused on the developing the low-bandgap donor polymers to further increase the OPVs performance [16–28]. The variable structures of low-bandgap conjugated polymers provided a possibility toward increasing the short circuit current density (J_{sc}) and the open circuit voltage (V_{oc}) [29–34] by modifying their highest occupied molecular orbital (HOMO) levels. 4,7-dithien-2-yl-2,1,3-benzothiadiazole (DTBT) has been comprehensively studied as building blocks in low-bandgap copolymers [35–41]. The thiophenes in the DTBT units could reduce the bandgap for the extending of the donor-acceptor conjugation and increasing of the planarity, as well as improve hole-transporting properties of the resulting copolymers [42]. Poly{[(2,7-(9-(2'-ethylhexyl)-9-hexyl-fluorene)-alt-[5,5-(-(4,7-di-2-thienyl-2,1,3-benzothiadiazole))}(PFDTBT) was introduced into OPVs as the electron donor polymer and exhibited a relatively high PCE of 2.2% when it was blended with $PC_{60}BM$. The solubility of PFDTBT was very poor with the number average molecular weight (M_n) of 4800, which limited the PCE of the corresponding devices [43]. Then, docecyl side chains were introduced onto the 9-positions of fluorene units to enhance the solubility of the copolymer poly{[(2,7-(9,9-didodecyl-fluorene)-alt-[5,5-(-(4,7-di-2-thienyl-2,1,3-benzothiadiazole))} (DiD-PFDTBT) and a

Received May 21, 2013; accepted August 28, 2013

E-mail: tgl@mail.hust.edu.cn, jianzhang@dicp.ac.cn

higher M_n (31000) was achieved. However, the distinctly steric hindrance of the side chains decreased the π-π stacking and subsequently reduced the charge mobility of DiD-PFDTBT, leading to a relatively lower PCE (1.4%) than that of PFDTBT [44]. Unbulky side chains with methyl groups located on the third and seventh carbon of octyl were applied to the fluorene units to prepare poly {[2,7-(9,9-bis-(3,7-dimethyl-octyl)-fluorene)]-alt-[5,5-(4,7-di-2-thienyl-2,1,3-benzothiadiazole)]} Bis(DMO-PFDTBT), which not only increased the solubility of the polymer but also decreased the steric effect between polymer chains. The resulting polymer exhibited a PCE up to 4.5% when it was blended with $PC_{70}BM$ [45].

To overcome the poor solubility of DTBT-based polymers, side chains were also introduced onto thiophenes of DTBT units. It was found that the side chains on the DTBT units not only affected their molecular weight, solubility and geometry of the corresponding polymers, but also determined their absorptions, energy levels, and film morphologies. Octyl groups were introduced into thiophenes at 3- or 4-positions of the DTBT units respectively to investigate their influence. The substituted on 4-positions of thiophenes exhibited a less steric hindrance than that on 3-positions. The corresponding polymer of 4-positions showed a triple PCE value of that with octyl substituted on 3-positions [8]. Charge mobility of the DTBT based low-bandgap polymers were also depend on the alkyl chains positions on thiophene and the polymers with substitutes on 4-positions provided higher mobility for its stronger intermolecular stacking than that on 3-positions [46].

To improve the charge mobility of the DTBT based polymer, nitrogen atoms were introduced into the 9-positions of fluorenes which provided carbazole-based polymer. Poly[*N*-9′-heptadecanyl-2,7-carbazole-alt-5,5-(4′,7′-di-2-thienyl-2′,1′,3′-ben-zothiadiazole)] (PCDTBT) was investigated as the donor material for its fully aromatic, which provided a better chemical and environmental stability. PCDTBT showed a relatively high PCE value of 3.6% when blended with $PC_{60}BM$ [47], and the PCE could be further improved to 6.1% by using the titanium oxide (TiO_x) layer as an optical spacer and hole blocker when the $PC_{70}BM$ was chosen as the electron acceptor [48].

According with the results of P3HT, molecular weight and polydispersity index (PDI) of the donor polymers are one of the key factors for the corresponding OPVs performances [49–53]. All the above studies of the DTBT-based polymers included both chemical structure and molecular effects. To obtain a clear outline how the chemical structures determined the device performances, it is urgent to exclude the influence of molecular weight when tuning the side chains and copolymerization units in the DTBT-based polymers, which will help to provide a general procedure for materials optimization. In this paper, five DTBT-based copolymers with comparable repeated units were prepared with varying copolymerization segments and hexyl side chains on thiophenes of DTBT units (Scheme 1). 3,7-dimethyl-octyls were chosen as the side chains on fluorenes or carbazoles for the copolymers without side chains substituted on DTBT to improve their solubility. All the absorptions, energy levels and the morphologies of resulting polymers, as well as their photovoltaic properties were studied with similar repeating units in the polymer backbone. Copolymer based on phenothiazine and DTBT were also employed. However, its molecular weight is much lower than the other four polymers for its poor solubility.

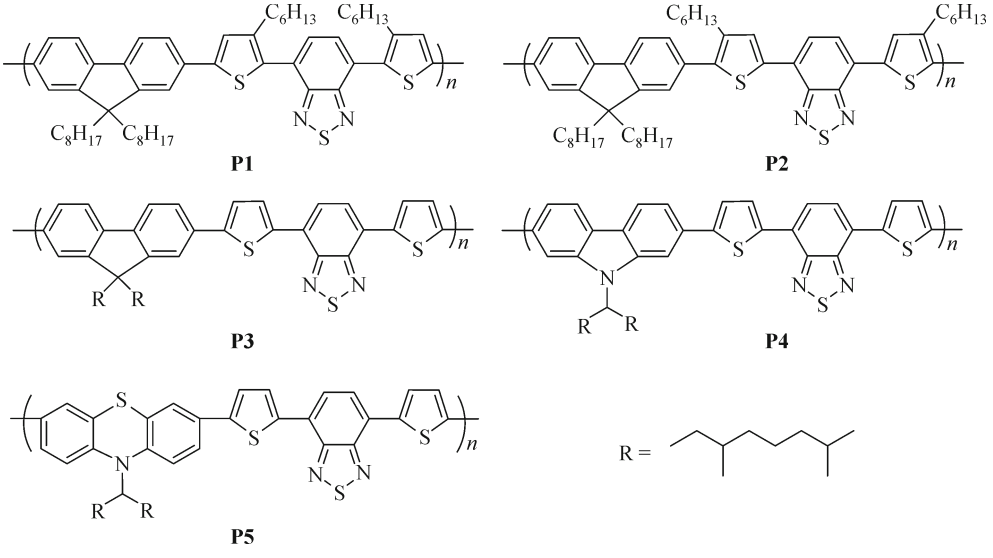

Scheme 1 Molecular structures of five DTBT based polymers

2 Experimental section

2.1 Materials

All reagents and solvents, unless otherwise specified, were obtained from Sigma-Aldrich or TCI chemical Co., and were used as received. Anhydrous tetrahydrofuran (THF) was distilled over sodium/diphenylketone under N_2 prior to use. All manipulations involving air-sensitive reagents were performed under an atmosphere of dry nitrogen. The 2,2'-(9,9-dioctyl-9H-fluorene-2,7-diyl)bis(4,4,5,5-tetramethyl-1,-3,2-dioxaborolane)(1) [54], 4,7-bis(5-bromothiophen-2-yl)benzo-2,1,3-thiadiazole (2) [54], 4,7-bis (5-bromo-3-hexylthiophen-2-yl)benzo-2,1,3-thiadiazole (4) [55], 2,6,12,16-tetramethylheptadecan-9-ol [56], P2 [56], and P3 [45] were synthesized according to literature procedures.

2.2 Synthesis of monomers

2.2.1 2,6,12,16-tetramethylheptadecan-9-yl 4-methylbenzenesulfonate (8)

P-toluenesulfonyl chloride (11.20 g, 58.75 mmol) in CH_2Cl_2 (50 mL) was added to the stirred solution of 2,6,12,16-tetramethylheptadecan-9-ol (12.18 g, 39.16 mmol), Et_3N (97.9 mmol, 13.75 mL) and $Me_3N{\cdot}HCl$ (3.74 g, 39.16 mmol) in CH_2Cl_2 (250 mL) in a 500 mL flask at 0 – 5°C, the mixture was stirred overnight. The organic phase was washed with water and brine, dried over magnesium sulfate and concentrated under reduced pressure. The crude product was purified by silica-gel column chromatography (hexanes/ethyl acetate = 10/1) to obtain colorless oil (15.6 g, yield: 81%). ^{1}H NMR (400 MHz, $CDCl_3$, ppm) δ: 7.79 (d, J = 8.1 Hz, 2H), 7.31 (d, J = 8.0 Hz, 2H), 4.51 (qt, J = 5.8 Hz, 1H), 2.43 (s, 3H), 1.55-1.49 (m, 4H), 1.12-1.09 (br, 32H), 0.86 (t, J = 6.6 Hz, 6H); ^{13}C NMR (400 MHz, $CDCl_3$, ppm): 144.24, 134.92, 129.61, 127.73, 85.30, 39.27, 36.97, 32.52, 31.74, 31.55, 27.94, 24.65, 22.64, 21.57, 19.42; *m/z*[m^+] 483.6 ; Calcd: 484.0.

2.2.2 10-(2,6,12,16-tetramethylheptadecan-9-yl)-10H-phenothiazine (10)

The NaH (1.15 g, 48 mmol) was dispersed in the dry THF (100 mL) and was added into the solution of 10H-phenothiazine (4.42 g, 21.2 mmol) in the dry THF (150 mL). After the mixture was refluxed for 1 h with stirring, 2,6,12,16-tetramethylheptadecan-9-yl-4-methylbenzenesulfonate (15.6 g, 32 mmol) in 100 mL dry THF was dropped to the solution within 1 h, and the reaction was stirred for overnight under refluxing. The mixture was quenched with water (200 mL), and extracted three times with hexane (300 mL). The combined organic fraction was dried over magnesium sulfate, and the solvent was removed under reduced pressure. The crude product was purified by silica-gel column chromatography (hexane as eluent) resulting a yellow oil (6.3 g, yield: 61%). ^{1}H NMR (400 MHz, $CDCl_3$, ppm) δ: 7.09 – 7.05 (m, 4H), 6.91 – 6.81 (m, 4H), 3.58 – 3.54 (m, J = 5.8 Hz, 1H), 2.07 (m, 2H), 1.79 (m, 2H), 1.49 – 1.08 (m, 20H), 0.87 – 0.81 (m, J = 5.2 Hz, 18H); ^{13}C NMR (400 MHz, $CDCl_3$, ppm): 145.49, 127.32, 126.87, 126.71, 122.44, 117.64, 64.89, 39.33, 37.36, 36.80, 34.66, 32.76, 32.01, 28.02, 24.77, 22.73,19.58; *m/z*[m^+] 494.8; Calcd: 494.3.

2.2.3 3,7-dibromo-10-(2,6,12,16-tetramethylheptadecan-9-yl)-10H-phenothiazine (11)

The solution of *N*-bromosuccinimide (17.00 g, 95.5 mmol) in dry dimethylformamide (DMF) (50 mL) was added dropwise into the mixture of 10-(2,6,12,16-tetramethylheptadecan-9-yl)-10H-phenothiazine (19.66 g, 39.8 mmol) in dry DMF (50 mL), the reaction was stirred overnight at room temperature, quenched with water, extracted with CH_2Cl_2 three times (450 mL), washed with brine, and dried over magnesium sulfate. The solvent was removed under reduced pressure and the crude residue was purified by silica-gel column chromatography (hexane as eluent) to give yellow color oil (17.09 g, yield: 66%). ^{1}H NMR (400 MHz, $CDCl_3$, ppm) δ: 7.20 – 7.16 (m, 4H), 6.72 (d, J = 5.8 Hz, 2H), 3.47 (m, J = 5.5 Hz, 1H), 1.98 (m, 2H), 1.81 (m, 2H), 1.78 – 1.03 (br, 20H), 0.83 (br, J = 6.6 Hz, 18H); ^{13}C NMR (400 MHz, $CDCl_3$, ppm): 144.30, 129.88, 129.57, 128.20, 118.76, 114.91, 65.32, 39.26, 37.26, 36.73, 34.59, 32.63, 31.91, 31.73, 27.98, 24.67,22.68, 19.97; *m/z*[m^+] 651.2; Calcd: 651.2.

2.2.4 10-(henicosan-11-yl)-3,7-bis(4,4,5,5-tetramethyl-1,3,2-diocaborolan-2-yl)-10-H-Phenothiazine (3)

N-butyllithium (16.0 mL, 30 mmol, 2.5 mol/L in hexane) was added dropwise to the solution of compound 11 (6.52 g, 10 mmol) in dried THF (150 mL) in a 250 mL flask at – 78°C. The mixture was stirred at – 78°C for 1 h and 2-iso-propoxy-4,4,5,5-tetramethyl-1,3,2-dioxaborolane (8.1 mL, 40 mmol) was added rapidly to the solution. After additional one hour at – 78°C, the resulting mixture was warmed to room temperature and stirred overnight. The mixture was poured into water, extracted with diethyl ether four times and dried over magnesium sulfate. The solvent was removed under reduced pressure and the residue was purified by silica-gel column chromatography (hexane as eluent, the silica–gel pretreatment with Et_3N) to obtain the title product as a yellow powder solid. (2.1 g, yield: 30%). ^{1}HNMR (400 MHz, C_6D_6, ppm) δ: 7.98 (s, 2H), 7.92 (d, J = 8.4 Hz, 2H), 6.95 (d, J = 8.2 Hz, 2H), 3.67 (m, J = 6.5 Hz, 1H), 1.99 (br, 2H), 1.83 (br, 2H), 1.48 – 1.07 (br, 44H), 0.79 – 0.72 (br, J = 6.0 Hz, 18H); ^{13}C NMR (400 MHz,

C_6D_6, ppm): 147.66, 133.74, 133.68, 125.74, 116.67, 83.63, 64.78, 39.25, 37.35, 36.76, 34.61, 32.63, 31.75, 27.94, 24.79, 22.68, 19.99, 19.48; *m/z*[m^+] 745.7; Calcd: 745.2.

2.2.5 2,7-dibromo-9-(2,6,12,16-tetramethylheptadecan-9-yl)-9H-carbazole (9)

A three neck flask fitted with an addition funnel and a magnetic stirring bar was charged with 2,7-dibromocarbazole (5.0 g, 10 mmol) and dried THF (150 mL). When the carbazole was completely dissolved, NaH (1.47 g, 61.5 mmol) was added to the solution, and refluxed for 1 h with stirring. Then the solution of compound 8 (15.0 g, 30.8 mmol) in dried THF (50 mL) was dropped into the mixture within 1 h, and refluxed overnight with stirring. The mixture was poured into distilled water (400 mL), and the aqueous layer was extracted with hexane three times, the combined organic fraction was dried with over magnesium sulfate and the solvent was removed under reduced pressure. The crude product was purified by column chromatography (silica-gel, hexane as eluent) resulting a colorless oil (7.5 g, yield: 78%). ^{1}H NMR (400 MHz, $CDCl_3$, ppm) δ: 7.88 (t, J = 8.6 Hz, 2H), 7.69 (s, 1H), 7.52 (s, 1H), 7.27 (br, 2H), 4.34 (m, J = 5.5 Hz, 1H), 2.16 (br, 2H), 1.91 (br, 2H), 1.13 (br, 20H), 0.81 (br, 18H); ^{13}C NMR (400 MHz, $CDCl_3$, ppm): 142.98, 139.44, 122.36, 121.47, 120.89, 119.89, 119.20, 114.51, 112.21, 57.48, 39.15, 36.73, 33.60, 32.54, 31.25, 30.66, 27.89, 19.64, 14.15; *m/z*[m^+] 619.5; Calcd: 620.2.

2.2.6 2,7-bis(4,4,5,5-tetramethyl-1,3,2-dioxaborolan-2-yl)-9-(2,6,12,16-tetramethylheptadecan-9-yl)-9H-carbazole (2)

N-butyllithium (7.5 mL, 12 mmol, 2.5 mol/L in hexane) was added dropwise to a solution of compound 9 (3.0 g, 4.8 mmol) in dry THF (150 mL) in a 250 mL flask at −78°C.The mixture was stirred at −78°C for 1 h and 2-iso-propoxy-4,4,5,5-tetramethyl-1,3,2-dioxaborolane (2.96 mL, 14.5 mmol) was added rapidly to the solution. After additional one hour at −78°C, the resulting was warmed to room temperature and stirred overnight. The mixture was poured into water, extracted with diethyl ether four times and dried over magnesium sulfate, the organic phase was removed under reduced pressure and the residue was purified by silica-gel column chromatography (CH_2Cl_2/hexane = 10:1 as eluent) to obtain a white solid (0.85 g, yield: 25%). ^{1}H NMR (400 MHz, $CDCl_3$, ppm) δ: 8.11 (br, 2H), 8.03 (s, 1H), 7.86 (s, 1H), 7.65 (d, J = 7.4 Hz, 2H), 4.63 (m, 1H), 2.31 (br, 2H), 1.96 (br, 2H), 1.41 (br, 24H), 1.14 (br, 20H), 0.79 (br, 18H); ^{13}C NMR (400 MHz, $CDCl_3$, ppm): 141.99, 138.68, 126.02, 124.76, 124.72, 124.58, 119.97, 119.70, 118.20, 115.44, 56.83, 39.18, 36.72, 33.62, 31.40, 31.12, 27.86, 24.74, 22.55, 19.61, 14.22; *m/z*[m^+] 713.6; Calcd: 714.2.

2.3 Synthesis of polymers

2.3.1 Poly[(9,9-dioctyl-fluoren)-alt-4,7-bis(3-hexyl-thiophene-2-yl)benzo-2,1,3-thiadia-zole] (PFDTBT-in, P1) is presented in detail as a representative example

In a 50 mL flask, compound (1) (0.3213 g, 0.5 mmol), compound (4) (0.3132 g, 0.5 mmol), tris(dibenzylideneacetone)dipalladium (20 mg), and postassium carbonate (1.3891 g, 10 mmol) were dissolved in degassed toluene (5 mL) and degassed deionized water (5 mL). After 4 days at 80°C, the polymer was obtained and precipitated in methanol/water (20:1). The polymer was filtered and washed with ethyl acetate, hexane, dichloromethane, chloroform on Soxhlet apparatus. The chloroform fraction was dried and characterized (370 mg, yield: 84%). ^{1}H NMR (400 MHz, CDCl3, ppm) δ: 7.75 (br, 6H), 7.65 (br, 2H), 7.43 (br, 2H), 2.77 (br, 4H), 2.08 (br, 4H), 1.75 (br, 4H), 1.36 – 1.11 (br, 36H), 0.87 – 0.73 (br, 12H).

2.3.2 Poly[(*N*-9'-2,6,12,-16-Tetramethyl-heptadecane-2,7-carbazole)-alt-5,5-(4',7'-di-2-thienyl-2',1',3′-benzothiadizaole)](TMHD-PCzDTBT, P4)

In a 50 mL flask, compound (2) (0.7137 g, 1 mmol), compound (5) (0.4582 g, 1 mmol), tris(dibenzylideneacetone)dipalladium (30 mg) and postassium carbonate (1.3891 g, 10 mmol) were dissolved in the mixture of degassed toluene (10 mL) and degassed deionized water (5 mL). After 50 h reaction at 80°C, the polymer was obtained and precipitated in methanol /water (20:1), filtered and washed on Soxhlet apparatus with ethyl acetate, hexane, dichloromethane, chloroform and o-dichlorobenzene. The o-dichlorobenzene fraction was dried and characterized (423 mg, yield: 49%). ^{1}H NMR (400 MHz, CDCl3, ppm) δ: 8.21 (br, 1H), 8.12 (br, 2H), 7.93 (br, 2H), 7.81 (br, 2H), 7.79 (br, 2H), 7.73 (br, 1H), 7.61 (br, 2H), 7.51 (br, 2H), 7.17 (br, 2H), 4.65 (br, 1H), 2.38 (br, 2H), 2.07 (br, 2H), 1.43-1.03 (br, 10H), 0.84-0.78 (br, 18H).

2.3.3 Poly[(*N*-10'-2,6,12,16-tetramethylheptadecane-3,7-phenothiazine)-alt-5,5-(4',7'-di-2-thienyl-2',1',3′-benzothiadizaole)] (TMHD-PPDTBT, P5)

In a 50 mL flask, compound (3) (0.3729 g, 0.5 mmol), compound (5) (0.2291 g, 0.5 mmol), tris(dibenzylideneacetone)dipalladium (20 mg), postassium carbonate (1.3891 g, 10 mmol) were dissolved in degassed toluene (10 mL) and degassed deionized water (5 mL). After 5 days at 80°C, the polymer was obtained and precipitated in methanol/water (20:1), The polymer was filtered and washed with ethyl acetate, hexane, dichloromethane, chloroform on Soxhlet apparatus. The chloroform fraction was dried and characterized (270 mg, yield: 70%). ^{1}H

NMR (400 MHz, CDCl3, ppm) δ: 8.10 (br, 2H), 7.83 (br, 2H), 7.53 (br, 2H), 7.42 (br, 4H), 6.95 (br, 2H), 3.65 (br, 1H), 2.13 (br, 2H), 1.86 (br, 2H) 1.47-1.26 (br, 20H), 0.89-0.84 (br, 18H).

2.4 Measurements

^{1}H-NMR and ^{13}CNMR spectra were recorded by Bruker-AF301 at 400 MHz. Mass spectra were carried out on an Agilent (1100 LC/MSD Trap). UV-visible absorption spectra were measured using a Shimadzu UV-VIS-NIR Spectrophotometer (UV-3600). Solid films of UV-vis spectra measurement were spin-coated on quatrz plate from o-dichlorobenzene solution. Thermogravimetric analysis (TGA) were undertaken using a PerkinElmer Instruments (Pyris1 TGA) under nitrogen atmosphere at a heating rate of 10°C/min. Cyclic voltammetry measurements were carried out in a conventional three electrode cell using a glassy carbon as working electrode in acetonitrile solution of 0.1 mol/L of tetrabutylammonium-hexafluorophosphate (Bu_4NPF_6) as the supporting electrolyte at scan rate of 50 mV/s. In each case, a glassy carbon working electrode were coated with a thin layer of polymer, a platinum wire as the counter electrode, and a sliver wire as the quasi-reference electrode were used, and $Ag/AgNO_3$ (0.1 mol/L) electrode were served as a reference electrode for all potentials quoted herein. The redox couple of ferrocene/ferrocenium ion (Fc/Fc^{+}) was used as external standard. The corresponding HOMO levels were calculated using $E_{ox/onset}$ for experiments in solid films. Polymer films on indium tin oxide (ITO) anode electrode were formed by spin-coating method. Atomic force microscopy (AFM) was obtained in tapping-mode using Veeco (DIMENSION 3100). Size chromatography was performed on Waters Alliance GPCV2000 with a refractive index detector. Columns: Water Styvagel GE*1, Water Styvagel HMW GE*2. The eluent was 1,2,4-trichlorobenzene. The working temperature was 135°C, and the resolution time was 2 h. The concentration of the sample was 0.5 mg/mL, which was filtered (filter: 0.2 μm) prior to the analysis. The molecular weight was calculated according to calibration with polystyrene standards. Devices characterization were carried out under AM 1.5 G irradiation with the intensity of 100 mW/cm^2 (Oriel 91160, 150 W) calibrated by a NREL certified standard silicon cell. Current versus potential (*I-V*) curves were recorded with a Keithley 2400 digital source meter. External quantum efficiencies (EQEs) were detected under monochromatic illumination (Oriel Cornerstone 260 1/4 m monochromatic equipped with Oriel 70613 NS QTH lamp), and the calibration of the incident light were performed with a monocrystalline silicon diode. The thickness of films were recorded by a profilometer (Alpha-Step 200, Tencor Instruments).

2.5 Fabrication of polymer photovoltaic cells

The structure of device was glass/ITO/PEDOT:PSS/Polymer:PCBM/Ca/Al. ITO-coated glass substrates were ultrasonically cleaned in detergent, deionized water, acetone, and isopropyl alcohol before the device fabrication. Then the substrates were treated with O_2 plasma for 5 min, and PEDOT:PSS (Baytron PVP Al 4083) was spin-coated onto ITO-coated glass substrate, followed by annealing at 150°C for 30 min. The thickness of the PEDOT:PSS layer was about 50 nm, as determined by a Dektak 6 M surface profilometer. Then, the active layer was prepared by spin coating from the solution of polymer and $PC_{60}BM$. The substrate was transfer into an evaporation chamber. A Ca layer (10 nm) was evaporated on the substrate under high vacuum (2×10^{-4} Pa), and then Al electrode (100 nm) was evaporated on the Ca layer under high vacuum as well. Post device annealing was carried out inside a nitrogen-filled glove box. The current-voltage characteristics of the photovoltaic cells were measured using a Keithley 2400 *I-V* measurement system. The measurement were conducted under the irradiation of AM 1.5 G simulated solar light (100 mW/cm^2), light intensity was adjusted by using a standard silicon photovoltaic cells with an optical filter.

3 Results and discussion

3.1 Synthesis and characterization of polymers

The synthesis of all the monomers and polymers are outlined in Scheme 2. Polymerizations were carried out by a Suzuki polymerization using the $Pd(PPh_3)_4$ as catalyst at 80°C for varying days. The M_n and PDI of copolymers were determined by high temperature gel permeation chromatography (GPC) with dichlorobenzene as eluent and polystyrene as a standard, and shown in Table 1. The M_n of P5 is 8600 that is much lower than other four polymers, which can be attributed to its poor solubility in toluene and precipitated during polymerization. The decomposition temperatures of these copolymers were investigated by TGA and shown in Fig. 1. P1, P2 and P3 exhibited 5% decomposition temperature over 400°C. P4 and P5 showed relatively low decomposition temperature (T_d) about 330°C. Neither obvious glass transition nor melting transition was observed for all the copolymers, indicating that the amorphous nature of the obtain polymers.

3.2 Optical and electrochemical properties of polymers

The UV-vis absorption spectra of polymer films were investigated, as shown in Fig. 2 and Table 1. All the copolymers exhibited two absorption peaks. The long

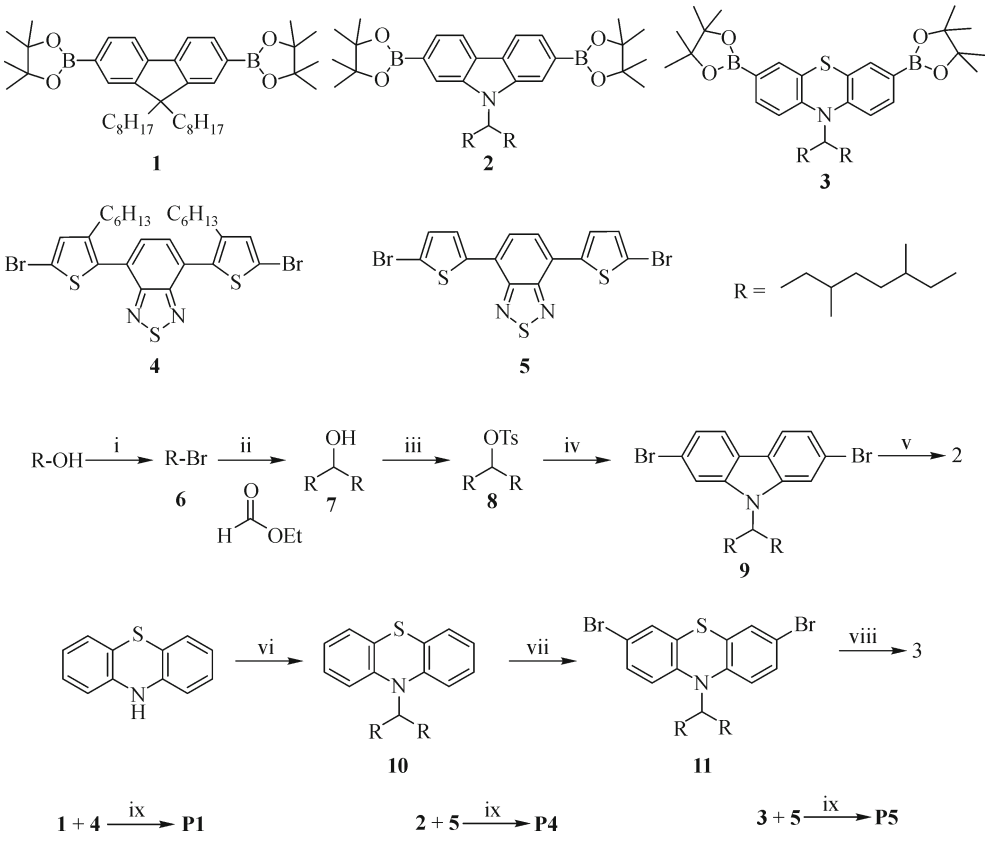

Scheme 2 Synthetic procedures of monomers and polymers

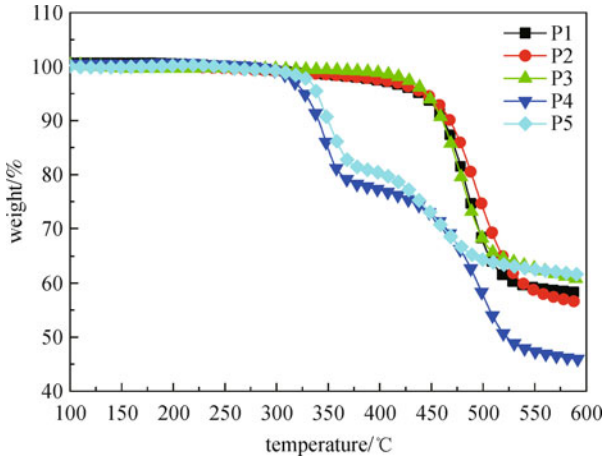

Fig. 1 TGA curves of five DBTB based copolymer at a scan rate of 10°C/min under a nitrogen atmosphere

wavelength absorption bands could be attributed to the intramolecular charge transfer (ICT). Compared with the ICT absorption of P1 at 486 nm, the absorption of P2 showed 44 nm red shift, which could be attributed to strong intermolecular stacking, indicating that alkyl side chains at the 4-positions of thiophenes displayed much less steric hindrance than that at the 3-positions and leading to a red-shift absorption of P2. For the polymer without hexyl side chains on DTBT units (P3), its long wavelength absorption located at 550 nm and exhibited 18 nm red-shift than P2, indicating stronger intermolecular π-stacking in P3 film. According to the above absorption spectra comparison of P1, P2, and P3, it clearly showed that alkyl substituted and its positions on DTBT units displayed strong steric effect and determined the intermolecular stacking. For P4, in which fluorene units were replaced by carbazoles, showed maxima absorptions at 400 and 562 nm respectively. There was 12 nm red shift of long wavelength absorption from P3 to P4, which may be attributed a stronger ICT for the atom replacing or better intermolecular π-stacking. P5 exhibited two absorption peaks situated at 390 and 564 nm. The long wavelength absorption was almost the same as P4 although the sulfur atom in phenothiazine was expected to show a strong electron donating ability. The reason may be originated from less flatness in phenothiazine than carbazole, and resulted in decreased intermolecular interaction.

The electrochemical properties of the polymers were characterized by cyclic voltammetry (CV) at room temperature. The CV curves were recorded referenced to an Ag/Ag^+ (0.01 mol/L of $AgNO_3$ in acetonitrile)

electrode, which was calibrated against the ferrocene/ferrocenium (Fc/Fc^+) redox couple (4.74 eV) below the vacuum level. The HOMO levels of the copolymers were obtained from the onset of oxidation potentials ($E_{ox,onset}$), as shown in Fig. 3. The LUMO levels of these five copolymers were about at −3.4~−3.5 eV, which was mainly dominated by the BT units (Table 1).

Calculated from CV, the energy gap of P2 was raised 0.12 eV than that of P1. The reason was that the alkyl chains were introduced at the 3-positions of the thienyl group, apparently reduced the electron delocalization and rendered a lower HOMO and higher LUMO energy levels. The HOMO level of P3 is −5.44 eV and its LUMO level was calculated from the bandgap results based on its absorption spectrum. P4 exhibited a similar HOMO level to P3, which indicated the carbazole units did not exhibit much stronger electron donating ability than fluorenes and the ICT absorption in the two copolymers were mainly contributed by the two thienyl groups in DTBT. So its 12 nm red-shift ICT absorption from P3 to P4 mainly originated from much stronger intermolecular aggregation in P4, which might result better π-π stacking and higher charge mobility. The HOMO and LUMO levels of P5 was about 0.2 eV higher than those of P4 for a stronger ICT from phenothiazine to 2,1,3-benzothiadiazole due to the existence of sulfur atoms. All the polymers expect for P5 had a relative low HOMO levels, indicating that the devices would have a relative large V_{oc}, which was proved by the results of the photovoltaic device performances.

3.3 Photovoltaic characteristics of polymer thin films

OPV devices were fabricated with the five polymers as the electron donors and the $PC_{60}BM$ as the electron acceptor to explore the effect of the side chains and backbone on the properties of DTBT based copolymer photovoltaic cells. The structure of devices were ITO/PEDOT:PSS (50 nm)/polymer:$PC_{60}BM$/Ca (10 nm)/Al (100 nm).

The solutions of polymer/$PC_{60}BM$ were spin-coated on PEDOT:PSS modified ITO glass with of 1,2-dichlorobenzene as the solvent. No additive was applied to simplify the comparison. Ratios of the different polymer/$PC_{60}BM$ had been optimized from 1:1, 1:2, 1:3, 1:4, and the best ratio was chosen as shown in Table 2. The thickness of the

Table 1 Molecular weight, PDI, and thermal properties, opticals and electrochemical properties of polymers

	Mn[a] /(kg·mol^{-1})	PDI	repeat unit	T_d[b] /°C	λ_{max} /nm	E_g^{opt} [c] /eV	HOMO [d] /eV	LUMO [e] /eV
P1	26.1	1.69	30	438.9	374/486	2.10	−5.53	−3.43
P2	28.8	1.71	33	443.6	372/530	1.98	−5.47	−3.49
P3	18.8	1.40	25	444.7	390/550	1.93	−5.44	−3.51
P4	16.6	2.49	22	327.2	400/562	1.85	−5.44	−3.59
P5	8.6	1.93	11	339.3	390/564	1.81	−5.18	−3.37

Notes: a) Determined by the GPC in dichlorobenzene using polystyrene as standards. M_n: number-average molecular weight; PDI: polydispersity index (M_w/M_n);
b) Temperature at 5% weight loss determined by TGA at a heating rate of 10°C/min under nitrogen;
c) Calculated from the absorption band edge of the copolymer film, $E_g^{opt} = 1240/\lambda_{edge}$;
d) Thin films in $CH_3CN/n\text{-}Bu_4NPF_6$, versus ferrocenium/ferrocene at 50 mV/s . HOMO value was estimated from the onset oxidation potential, and e) LUMO value was estimated from LUMO = HOMO − E_g^{opt}

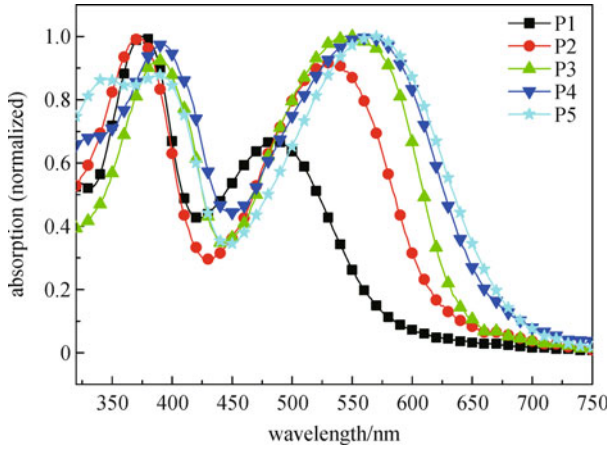

Fig. 2 UV-vis absorption spectra of the thin film of polymers

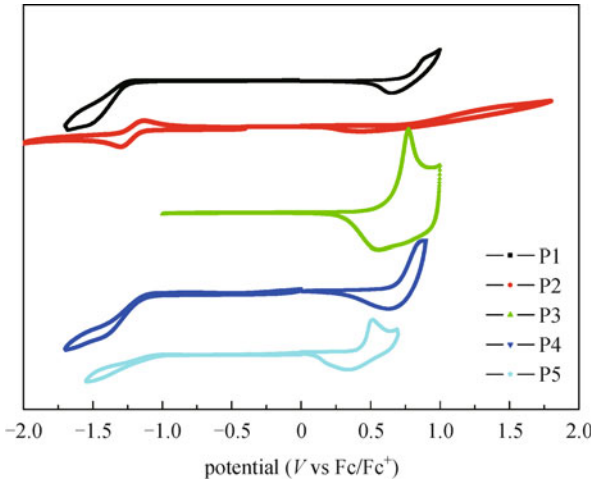

Fig. 3 Cyclic voltammetry of polymers film coated on a glass carbon electrode in Bu_4NPF_4/CH_3CN solution

active layers, around 60 – 70 nm, was also optimized for all polymer films. The resulting films were dried under vacuum at room temperature and then annealed for 15 min. The optimized annealing temperatures for the five polymers were listed in Table 2. Then cathodes were deposited onto active layers at 2×10^{-4} Pa with a metal mask. The *J-V* characteristics of photovoltaic cells were shown in Fig. 4 and the J_{sc}, fill factor (*FF*), and PCE of the devices were summarized in Table 2.

Compared with devices of P1, the devices of P2 showed doubled J_{sc} and PCE value, which is consistent with the result that P2 had stronger intermolecular aggregation than P1 for the different position of hexyl. And due to the same reason, P3 showed much higher J_{sc} and PCE than P2. When the fluorene units were replaced by carbazoles, P4 exhibited a little higher PCE than that of P3, which originated from the increased J_{sc} although its V_{oc} and *FF* were lower than those of P3. The increased J_{sc} in devices of P4 was contributed by its strong intermolecular stacking in films. P5 showed much lower PCE than P4 for the reasons of poor solubility and J_{sc}. All the devices had shown a relatively higher V_{oc} value from 0.76 to 0.87 V except for P5. According to the above results, the PCE of the five DTBT-based polymers were mainly determined by the J_{sc} of the devices, as shown in Table 2.

To study the contribution of polymer absorption to J_{sc}, the external quantum efficiency (EQE) of device based on the copolymers were measured under the illumination of monochromatic light as showed in Fig. 5. The maximum EQEs of P3 and P4 were much higher than those of P1 and P2, agreeing with the devices results.

3.4 Morphology

The nanoscale morphologies for polymer/PCBM films were studied using tapping-mode atomic force microscopy (AFM). Phase images (top) and surface topography (under) were taken for each film and shown in Fig. 6. Distinctly different morphologies of polymer:PCBM blend films were observed in their phase images, indicating that the active layer morphology was strongly affected by the structures of the polymers. The root mean square roughnesses (R_{rms}) of these five polymers were 0.26, 0.32, 0.49, 0.45 and 0.26 nm respectively, which indicated that the stronger intermolecular stacking would exhibit large size of phase separations and R_{rms}. This agreed with corresponding devices performances.

4 Conclusions

Five DTBT based copolymers with controlled molecular weight were synthesized and characterized to explore the

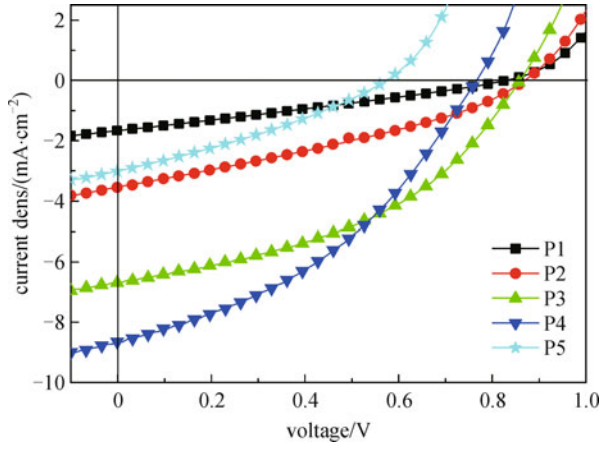

Fig. 4 *J-V* characteristics of photovoltaic cells of five polymers

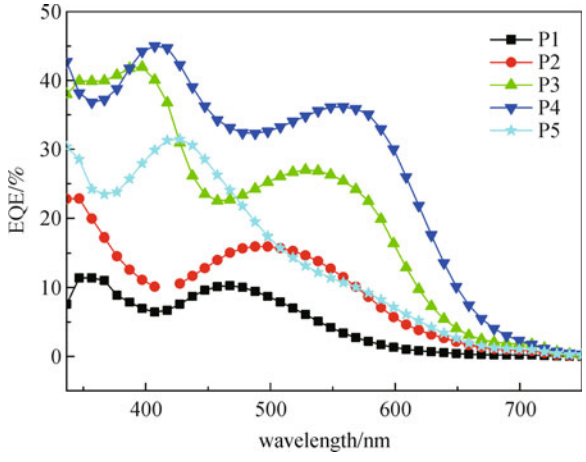

Fig. 5 External quantum efficiency (EQE) of PSCs based on five polymers

Table 2 Optimized device characteristics of five DTBT based copolymers

	polymer:$PC_{60}BM$ (weight ratio)	annealing temperature /°C	thickness /nm	J_{sc} /(mA·cm^{-2})	V_{oc} /V	*FF*	PCE /%
P1	1:4	60	74	1.65	0.82	0.28	0.38
P2	1:3	70	71	3.51	0.87	0.29	0.69
P3	1:3	130	73	6.67	0.86	0.43	2.47
P4	1:2	80	66	8.65	0.76	0.40	2.60
P5	1:2	100	56	2.98	0.57	0.32	0.54

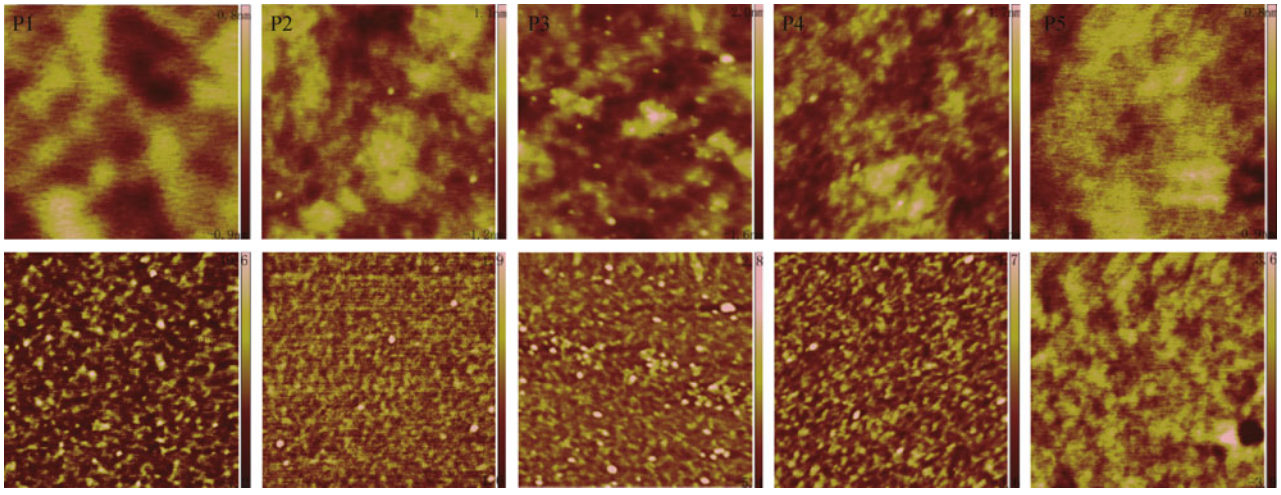

Fig. 6 AFM (5 μm × 5 μm) topography and phase images of five polymers

influence of side chains and backbone structure on the properties of absorption spectrums, energy levels, and photovoltaic devices. Strong steric hindrance would be produced when side chains were introduced onto the thiophenes in DTBT units, which also exhibited position dependence when modifying the side chains from 3- to 4-positions. For the polymer without alkyl substituted on DTBT, the polymer showed stronger intermolecular stacking and lower bandgap. When the copolymerization units were changed from fluorene to carbazole, the red-shift ICT absorption in carbazole copolymer was mainly attributed to its better π-π stacking. And for all the five DTBT-based copolymers, the PCE of their corresponding devices mainly depended on their J_{sc}, which were determined by the intermolecular stacking of the donor polymers and had also been proved by their morphology results.

Acknowledgements Financial support by the National Natural Science Foundation of China (Grant Nos. 51073063 and 20904057) and Open Project of State Key Laboratory for Supramolecular Structure and Materials (No. SKLSSM201129) of Jilin university are gratefully acknowledged. J. Zhang thanks the support by 100 Talents Programme of the Chinese Academy of Science.

References

1. Yu G, Gao J, Hummelen J C, Wudl F, Heeger A J. Polymer photovoltaic cells: enhanced efficiencies via a network of internal donor-acceptor heterojunctions. Science, 1995, 270(5243): 1789–1791
2. Brabec C J, Sariciftci N S, Hummelen J C. Plastic solar cells. Advanced Functional Materials, 2001, 11(1): 15–26
3. Coakley K M, McGehee M D. Conjugated polymer photovoltaic cells. Chemistry of Materials, 2004, 16(23): 4533–4542
4. Günes S, Neugebauer H, Sariciftci N S. Conjugated polymer-based organic solar cells. Chemical Reviews, 2007, 107(4): 1324–1338
5. Ma W, Yang C, Gong X, Lee K, Heeger A J. Thermally stable, efficient polymer solar cells with nanoscale control of the interpenetrating network morphology. Advanced Functional Materials, 2005, 15(10): 1617–1622
6. Reyes-Reyes M, Kim K, Carroll D L. High-efficiency photovoltaic devices based on annealed poly(3-hexylthiophene) and 1-(3-methoxycarbonyl)-propyl-1-phenyl-(6,6)C_{61}blends. Applied Physics Letters, 2005, 87(8): 083506–083508
7. Qin R P, Li W W, Li C H, Du C, Veit C, Schleiermacher H F, Andersson M, Bo Z, Liu Z P, Inganäs O, Wuerfel U, Zhang F L. A planar copolymer for high efficiency polymer solar cells. Journal of the American Chemical Society, 2009, 131(41): 14612–14613
8. Peet J, Kim J Y, Coates N E, Ma W L, Moses D, Heeger A J, Bazan G C. Efficiency enhancement in low-bandgap polymer solar cells by processing with alkane dithiols. Nature Materials, 2007, 6(7): 497–500
9. Thompson B C, Fréchet J M J. Polymer-fullerene composite solar cells. Angewandte Chemie International Edition, 2007, 47(1): 58–77
10. Kim Y, Cook S, Tuladhar S M, Choulis S A, Nelson J, Durrant J R, Bradley D D C, Giles M, McCulloch I, Ha C S, Ree M. A strong regioregularity effect in self-organizing conjugated polymer films and high-efficiency polythiophene:fullerene solar cells. Nature Materials, 2006, 5(3): 197–203
11. Li G, Shrotriya V, Huang J S, Yao Y, Moriarty T, Emery K, Yang Y. High-efficiency solution processable polymer photovoltaic cells by self-organization of polymer blends. Nature Materials, 2005, 4(11): 864–868
12. Shi C J, Yao Y, Yang Y, Pei Q B. Regioregular copolymers of 3-alkoxythiophene and their photovoltaic application. Journal of the American Chemical Society, 2006, 128(27): 8980–8986
13. Campoy-Quiles M, Ferenczi T, Agostinelli T, Etchegoin P G, Kim Y, Anthopoulos T D, Stavrinou P N, Bradley D D C, Nelson J. Morphology evolution via self-organization and lateral and vertical diffusion in polymer:fullerene solar cell blends. Nature Materials, 2008, 7(2): 158–164
14. Zhao G J, He Y J, Li Y F. 6.5% efficiency of polymer solar cells

based on poly(3-hexylthiophene) and indene-C_{60} bisadduct by device optimization. Advanced Materials, 2010, 22(39): 4355–4358

15. Chang C Y, Wu C E, Chen S Y, Cui C H, Cheng Y J, Hsu C S, Wang Y L, Li Y F. Enhanced performance and stability of a polymer solar cell by incorporation of vertically aligned, cross-linked fullerene nanorods. Angewandte Chemie International Edition, 2011, 50(40): 9386–9390
16. He F, Wang W, Chen W, Xu T, Darling S B, Strzalka J, Liu Y, Yu L P. Tetrathienoanthracene-based copolymers for efficient solar cells. Journal of the American Chemical Society, 2011, 133(10): 3284–3287
17. Piliego C, Holcombe T W, Douglas J D, Woo C H, Beaujuge P M, Fréchet J M J. Synthetic control of structural order in *N*-alkylthieno [3,4-c]pyrrole-4,6-dione-based polymers for efficient solar cells. Journal of the American Chemical Society, 2010, 132(22): 7595–7597
18. Chen H Y, Hou J H, Zhang S Q, Liang Y Y, Yang G W, Yang Y, Yu L P, Wu Y, Li G. Polymer solar cells with enhanced open-circuit voltage and efficiency. Nature Photonics, 2009, 3(11): 649–653
19. Price S C, Stuart A C, Yang L Q, Zhou H X, You W. Fluorine substituted conjugated polymer of medium band gap yields 7% efficiency in polymer-fullerene solar cells. Journal of the American Chemical Society, 2011, 133(12): 4625–4631
20. Kim J Y, Lee K, Coates N E, Moses D, Nguyen T Q, Dante M, Heeger A J. Efficient tandem polymer solar cells fabricated by all-solution processing. Science, 2007, 317(5835): 222–225
21. Wang E, Hou L T, Wang Z Q, Hellström S, Zhang F L, Inganäs O, Andersson M R. An easily synthesized blue polymer for high-performance polymer solar cells. Advanced Materials, 2010, 22(46): 5240–5244
22. Amb C M, Chen S, Graham K R, Subbiah J, Small C E, So F, Reynolds J R. Dithienogermole as a fused electron donor in bulk heterojunction solar cells. Journal of the American Chemical Society, 2011, 133(26): 10062–10065
23. Chang C Y, Wu C E, Chen S Y, Cui C H, Cheng Y J, Hsu C S, Wang Y L, Li Y F. Enhanced performance and stability of a polymer solar cell by incorporation of vertically aligned, cross-linked fullerene nanorods. Angewandte Chemie International Edition, 2011, 50(40): 9386–9390
24. Jin J K, Choi J K, Kim B J, Kang H B, Yoon S C, You H, Jung H T. Synthesis and photovoltaic performance of low-bandgap polymers on the basis of 9,9-dialkyl-3,6-dialkyloxysilafluorene. Macromolecules, 2011, 44(3): 502–511
25. Peng Q, Liu X J, Su D, Fu G W, Xu J, Dai L M. Novel benzo[1,2-b:4,5-b']dithiophene-benzothiadiazole derivatives with variable side chains for high-performance solar cells. Advanced Materials, 2011, 23(39): 4554–4558
26. Huo L J, Guo X, Zhang S Q, Li Y F, Hou J H. PBDTTTZ: a broad band gap conjugated polymer with high photovoltaic performance in polymer solar cells. Macromolecules, 2011, 44(11): 4035–4037
27. Dou L T, You J B, Yang J, Chen C C, He Y J, Murase S, Moriarty T, Emery K, Li G, Yang Y. Tandem polymer solar cells featuring a spectrally matched low-bandgap polymer. Nature Photonics, 2012, 6(3): 180–185
28. Li G, Zhu R, Yang Y. Polymer solar cells. Nature Photonics, 2012, 6 (3): 153–161
29. Scharber M C, Mühlbacher D, Koppe M, Denk P, Waldauf C, Heeger A J, Brabec C J. Design rules for donors in bulk-heterojunction solar cells—towards 10% energy-conversion efficiency. Advanced Materials, 2006, 18(6): 789–794
30. Blouin N, Michaud A, Gendron D, Wakim S, Blair E, Neagu-Plesu R, Belletête M, Durocher G, Tao Y, Leclerc M. Toward a rational design of poly(2,7-carbazole) derivatives for solar cells. Journal of the American Chemical Society, 2008, 130(2): 732–742
31. Huo L J, Hou J H, Chen H Y, Zhang S Q, Jiang Y, Chen T L, Yang Y. Bandgap and molecular level control of the low-bandgap polymers based on 3,6-dithiophen-2-yl-2,5-dihydropyrrolo[3,4-c] pyrrole-1,4-dione toward highly efficient polymer solar cells. Macromolecules, 2009, 42(17): 6564–6571
32. Liang Y Y, Feng D Q, Wu Y, Tsai S T, Li G, Ray C, Yu L P. Highly efficient solar cell polymers developed via fine-tuning of structural and electronic properties. Journal of the American Chemical Society, 2009, 131(22): 7792–7799
33. Zoombelt A P, Fonrodona M, Wienk M M, Sieval A B, Hummelen J C, Janssen R A J. Photovoltaic performance of an ultrasmall band gap polymer. Organic Letters, 2009, 11(4): 903–906
34. Mondal R, Ko S, Norton J E, Miyaki N, Becerril H A, Verploegen E, Toney M F, Bredas J L, McGehee M D, Bao Z N. Molecular design for improved photovoltaic efficiency: band gap and absorption coefficient engineering. Journal of Materials Chemistry, 2009, 19 (39): 7195–7197
35. Dhanabalan A, Van Duren J K J, Van Hal P A, Van Dongen J L J, Janssen R A J. Synthesis and characterization of a low bandgap conjugated polymer for bulk heterojunction photovoltaic cells. Advanced Functional Materials, 2001, 11(4): 255–262
36. Boudreault P L T, Michaud A, Leclerc M. A new poly(2,7-Dibenzosilole) derivative in polymer solar cells. Macromolecular Rapid Communications, 2007, 28(22): 2176–2179
37. Song S, Jin Y, Kim S H, Moon J, Kim K, Kim J Y, Park S H, Lee K, Suh H. Stabilized polymers with novel indenoindene backbone against photodegradation for LEDs and solar cells. Macromolecules, 2008, 41(20): 7296–7305
38. Moulé A J, Tsami A, Bünnagel T W, Forster M, Kronenberg N M, Scharber M, Koppe M, Morana M, Brabec C J, Meerholz K, Scherf U. Two novel cyclopentadithiophene-based alternating copolymers as potential donor components for high-efficiency bulk-heterojunction-type solar cells. Chemistry of Materials, 2008, 20 (12): 4045–4050
39. Liao L, Dai L M, Smith A, Durstock M, Lu J P, Ding J F, Tao Y. Photovoltaic-active dithienosilole-containing polymers. Macromolecules, 2007, 40(26): 9406–9412
40. Zhou E, Nakamura M, Nishizawa T, Zhang Y, Wei Q S, Tajima K, Yang C H, Hashimoto K. Synthesis and photovoltaic properties of a novel low band gap polymer based on *N*-substituted dithieno[3,2-b:2′,3′-d]pyrrole. Macromolecules, 2008, 41(22): 8302–8305
41. Wang M, Hu X W, Liu P, Li W, Gong X, Huang F, Cao Y. Donor-acceptor conjugated polymer based on naphtho[1,2-c:5,6-c]bis [1,2,5]thiadiazole for high-performance polymer solar cells. Journal of the American Chemical Society, 2011, 133(25): 9638–9641
42. Zhou H X, Yang L Q, Xiao S Q, Liu S B, You W. Donor–acceptor

polymers incorporating alkylated dithienylbenzothiadiazole for bulk heterojunction solar cells: pronounced effect of positioning alkyl chains. Macromolecules, 2009, 43(2): 811–820

43. Svensson M, Zhang F, Veenstra S C, Verhees W J H, Hummelen J C, Kroon J M, Inganäs O, Andersson M R. High-performance polymer solar cells of an alternating polyfluorene copolymer and a fullerene derivative. Advanced Materials, 2003, 15(12): 988–991
44. Inganäs O, Svensson M, Zhang F, Gadisa A, Persson N K, Wang X, Andersson M R. Low bandgap alternating polyfluorene copolymers in plastic photodiodes and solar cells. Applied Physics A, 2004, 79 (1): 31–35
45. Chen M H, Hou J H, Hong Z, Yang G W, Sista S, Chen L M, Yang Y. Efficient polymer solar cells with thin active layers based on alternating polyfluorene copolymer/fullerene bulk heterojunctions. Advanced Materials, 2009, 21(42): 4238–4242
46. Lee S K, Cho S, Tong M, Seo J H, Heeger A J. Effects of substituted side-chain position on donor–acceptor conjugated copolymers. Journal of Polymer Science Part A: Polymer Chemistry, 2011, 49 (8): 1821–1829
47. Blouin N, Michaud A, Leclerc M. A low-bandgap poly(2,7-carbazole) derivative for use in high-performance solar cells. Advanced Materials, 2007, 19(17): 2295–2300
48. Park S H, Roy A, Beaupre S, Cho S, Coates N, Moon J S, Moses D, Leclerc M, Lee K, Heeger A J. Bulk heterojunction solar cells with internal quantum efficiency approaching 100%. Nature Photonics, 2009, 3(5): 297–302
49. Kline R J, McGehee M D, Kadnikova E N, Liu J S, Fréchet J M J, Toney M F. Dependence of regioregular poly(3-hexylthiophene) film morphology and field-effect mobility on molecular weight. Macromolecules, 2005, 38(8): 3312–3319
50. Schilinsky P, Asawapirom U, Scherf U, Biele M, Brabec C J. Influence of the molecular weight of poly(3-hexylthiophene) on the performance of bulk heterojunction solar cells. Chemistry of Materials, 2005, 17(8): 2175–2180
51. Koppe M, Brabec C J, Heiml S, Schausberger A, Duffy W, Heeney M, McCulloch I. Influence of molecular weight distribution on the gelation of P3HT and its impact on the photovoltaic performance. Macromolecules, 2009, 42(13): 4661–4666
52. Osaka I, Saito M, Mori H, Koganezawa T, Takimiya K. Drastic change of molecular orientation in a thiazolothiazole copolymer by molecular-weight control and blending with $PC_{61}BM$ leads to high efficiencies in solar cells. Advanced Materials, 2012, 24(3): 425–430
53. Müller C, Wang E, Andersson L M, Tvingstedt K, Zhou Y, Andersson M R, Inganäs O. Influence of molecular weight on the performance of organic solar cells based on a fluorene derivative. Advanced Functional Materials, 2010, 20(13): 2124–2131
54. Chu T Y, Alem S, Tsang S W, Tse S C, Wakim S, Lu J P, Dennler G, Waller D, Gaudiana R, Tao Y. Morphology control in polycarbazole based bulk heterojunction solar cells and its impact on device performance. Applied Physics Letters, 2011, 98(25): 253301–253303
55. Admassie S, Inganäs O, Mammo W, Perzon E, Andersson M R. Electrochemical and optical studies of the band gaps of alternating polyfluorene copolymers. Synthetic Metals, 2006, 156(7–8): 614–623
56. Koeckelberghs G, Cremer L D, Persoons A, Verbiest T. Influence of the substituent and polymerization methodology on the properties of chiral poly(dithieno[3,2-b:2′,3′-d]pyrrole)s. Macromolecules, 2007, 40(12): 4173–4181